NASA Technical Memorandum 87594

STRESS-INTENSITY FACTORS FOR CIRCUMFERENTIAL SURFACE CRACKS IN PIPES AND RODS UNDER TENSION AND BENDING LOADS

I. S. Raju and J. C. Newman, Jr.

August 1985

NASA
National Aeronautics and
Space Administration

Langley Research Center
Hampton, Virginia 23665

STRESS-INTENSITY FACTORS FOR CIRCUMFERENTIAL SURFACE CRACKS IN PIPES AND RODS UNDER TENSION AND BENDING LOADS

I. S. Raju* and J. C. Newman, Jr.**
NASA Langley Research Center
Hampton, Virginia 23665

SUMMARY

The purpose of this paper is to present stress-intensity factors for a wide range of nearly semi-elliptical surface cracks in pipes and rods. The surface cracks were oriented on a plane normal to the axis of pipes or rods. The configurations were subjected to either remote tension or bending loads. For pipes, the ratio of crack depth to crack length (a/c) ranged from 0.6 to 1; the ratio of crack depth to wall thickness (a/t) ranged from 0.2 to 0.8; and the ratio of internal radius to wall thickness (R/t) ranged from 1 to 10. For rods, the ratio of crack depth to crack length also ranged from 0.6 to 1; and the ratio of crack depth to rod diameter (a/D) ranged from 0.05 to 0.35. These particular crack configurations were chosen to cover the range of crack shapes (a/c) that have been observed in experiments conducted on pipes and rods under tension and bending fatigue loads. The stress-intensity factors were calculated by a three-dimensional finite-element method. The finite-element models employed singularity elements along the crack front and linear-strain elements elsewhere. The models had about 6500 degrees of freedom. The stress-intensity factors were evaluated using a nodal-force method.

The present results were compared with other analytical and experimental results for some of the crack configurations. The results generally agreed within 10 percent.

---

*Senior Scientist, Analytical Services & Materials, Inc., Tabb, VA.
**Senior Scientist, Materials Division.

The present results will be useful to predict crack-growth rates and fracture strengths, to design structural components, and to establish inspection intervals.

INTRODUCTION

Surface cracks can occur in many structural components. Circumferential surface cracks can cause premature failure of landing gear of aircraft piping, bolts, pins, and reinforcements which employ cylindrical shaped components. Accurate stress analyses of these surface-cracked components are needed for reliable prediction of crack-growth rates and fracture strengths. However, because of the complexities of such problems, exact solutions are not available.

Some investigators have used experimental or approximate analytical methods to obtain stress-intensity factors for surface cracks in rods under tension and bending loads. The stress-intensity factors for a circumferential surface crack growing in a rod under remote uniform tension was obtained experimentally by Wilhem, et al. [1] using the James-Anderson procedure [2]. Their results show that the surface cracks intersect the outer surface of the rod at nearly right angles. Athanassiadis, et al. [3], (boundary-integral method) and Nezu, et al. [4], (finite-element method) used analytical methods to obtain stress-intensity factors for circumferential surface cracks of various shapes in rods. Their surface-crack shapes were chosen to agree with their experimental observations. In some of the experiments of Reference 4, however, the surface cracks did not intersect the outer surface at right angles. Residual stresses at the outer surface could have altered the crack shape near the free surface. Trantina, et al. [5] conducted an elastic and an elastic-plastic finite-element analysis of a small surface crack in a rod

under tension loading. They assumed that cracks intersected the outer surface at right angles.

Much less research has been conducted on circumferential surface cracks in hollow cylinders or pipes than on rods. Delale and Erdogan [6] and German, et al. [7] obtained stress-intensity factors for interior and exterior circumferential surface cracks using the line-spring model. Recently, Forman and Shivakumar [8] studied the fatigue-crack growth behavior of circumferential surface cracks in rods and pipes. Most of their experimental results did indicate that surface cracks intersect the free surfaces at about right angles.

This paper presents stress-intensity factors calculated with a three-dimensional finite-element analysis for a wide range of nearly semi-elliptical surface cracks in pipes and rods. The surface cracks were oriented on a plane normal to the axis of pipes or rods, as shown in Figure 1. The crack configurations were assumed to be such that the crack fronts intersect the free surface at right angles. The pipe and rod were subjected to either remote tension or bending loads. For pipes, the ratio of crack depth to crack length ranged from 0.6 to 1; the ratio of crack deptn to wall thickness ranged from 0.2 to 0.8; and the ratio of internal radius to wall thickness was 1 to 10. For rods, the ratio of crack depth to crack length also ranged from 0.6 to 1; and the crack configurations were chosen to cover the range of crack shapes that have been observed in experiments conducted on pipes and rods under tension and bending fatigue loads. The stress-intensity factors were calculated by a nodal-force method [9-11]. The present results were compared with other analytical and experimental results from the literature for some of the crack configurations.

SYMBOLS

a	depth of surface crack
c	half-arc length of surface crack
D	outer diameter of pipe and rod
F	stress-intensity boundary-correction factor
F_A	boundary-correction factor at maximum depth point on surface crack ($\phi = \pi/2$)
F_B	boundary-correction factor at intersection point of crack and outer surface
h	half-length of pipe and rod
K	stress-intensity factor (mode I)
K_A	stress-intensity factor at maximum depth point on surface crack ($\phi = \pi/2$)
Q	shape factor for elliptical crack
R	internal radius of pipe
S_b	remote bending stress on outer fiber
S_t	remote uniform-tension stress
t	wall thickness of pipe
x,y	Cartesian coordinate system
ν	Poisson's ratio
ϕ	parametric angle of ellipse

Superscript

$'$	primes denote quantities associated with surface crack in flat plate

THREE-DIMENSIONAL FINITE-ELEMENT ANALYSIS

A three-dimensional finite-element analysis was used to calculate the mode I stress-intensity factor variations along the crack front for a circumferential surface crack in the pipe and rod shown in Figures 1(a) and 1(b), respectively. The pipe and rod was subjected to either remote tension or

bending loads. In this analysis, Poisson's ratio (ν) was assumed to be 0.3. The shapes of the surface cracks were nearly but not exactly semi-elliptical. These crack shapes were generated using a conformal transformation as described in the appendix.

Figures 2(a) and 2(b) show typical finite-element models for a circumferential surface crack in a pipe and rod, respectively. The finite-element models employ singularity elements along the crack front and linear-strain elements elsewhere. The models had about 6500 degrees of freedom. Stress-intensity factors were evaluated from a nodal-force method. Details of the formulation of these types of elements and of the nodal-force method are given in References 9-11 and are not repeated here. Details on the development of the finite-element models are given in the appendix.

Loading

Two types of loads were applied to the finite-element models of the surface-cracked pipe and rod: remote uniform-tension and remote bending. The remote uniform-tension stress is S_t and the remote outer-fiber bending stress is S_b. The bending stress S_b, in Figure 3, is calculated at the origin of the surface crack ($x = y = 0$ in Fig. 4) without the crack being present.

Stress-Intensity Factor

The tension and bending loads only cause mode I deformations. The mode I stress-intensity factor K for any point along the surface-crack was taken to be

$$K = S_1 \sqrt{\frac{a}{\pi Q}}\, F \qquad (1)$$

where the subscript i denotes either tension load ($i = t$) or bending load ($i = b$), and Q, the shape factor for an ellipse, is given by the square of the complete elliptic integral of the second kind. The half-length of the pipe and rod, h, was chosen large enough to have a negligible effect on stress intensity ($h/D \geq 10$). Values for F, the boundary-correction factor, were claculated along the crack front for various combinations of parameters (a/t, a/c, R/t, and ϕ for a crack in a pipe; and a/c, a/D, and ϕ for a crack in a rod). The crack dimensions and parametric angle, ϕ, are defined in Figure 4. The range of crack shapes (a/c) and of sizes (a/t or a/D) analyzed are shown in Figures 5 and 6 for the pipe and rod, respectively.

The empirical expressions for Q used in this paper were developed by Rawe (see Ref. 11) and are

$$Q = 1 + 1.464(a/c)^{1.65} \text{ for } a/c \leq 1 \tag{2a}$$

$$Q = 1 + 1.464(c/a)^{1.65} \text{ for } a/c > 1 \tag{2b}$$

RESULTS AND DISCUSSION

In the following sections, stress-intensity factors for various shape surface cracks in pipes and rods subjected to tension and bending loads are presented. Tables 1-3 give the normalized stress-intensity factors, $K/S\sqrt{\pi a/Q}$, at the maximum depth point (A) and at the point which the crack intersects the free surface (B). Figures 7-12 show the variation in normalized stress-intensity factors, as a function of the parametric angle ($2\phi/\pi$) for various crack shapes (a/c), crack size (a/t or a/D), and radius of the pipe (R/t).

Pipes Under Tension Loads

Figure 7 shows the normalized stress-intensity factors as a function of the parametric angle (ϕ) for a pipe ($R/t = 2$) subjected to remote tension with a semi-circular crack ($a/c = 1$) for various values of a/t. For this crack shape, the maximum normalized stress-intensity factor occurred at the point where the crack meets the free surface (point B). For all of the a/c ratios considered (from 1 to 0.6), larger values of a/t always gave larger normalized stress-intensity factors.

For an a/c ratio of 0.8 and a/t less than or equal to 0.5, the normalized stress-intensity factors at the deepest point and at the free surface are nearly the same (see Table 1). On the other hand, for an a/c ratio of 0.6, the maximum normalized stress-intensity factors occurred at the point of maximum depth ($\phi = \pi/2$).

Figure 8 shows the normalized stress-intensity factors for a surface crack with $a/c = 0.8$ and $a/t = 0.5$ in pipes with R/t ratios of 1 and 10. (The results for $R/t = 2$ and 4 lie in between those for $R/t = 1$ and 10 and are not shown for clarity.) For this configuration, the effect of varying R/t is insignificant. However, for cracks with $a/c = 0.6$ and $a/t = 0.8$, R/t has a significant effect on the normalized stress-intensity factors, as shown in Figure 9. The values at the deepest point ($\phi = \pi/2$) are affected more than those at the free surface. Figure 9 shows that lower R/t values gave higher stress-intensity factors. However, the differences between the stress-intensity factors are less for larger values of R/t. Thus the effect of R/t diminishes for pipes with larger R/t values.

In summary, the effect of the curvature of the pipe (R/t) is to elevate the stress-intensity factors compared to a flat plate ($R/t = \infty$). The effect is more pronounced at the deepest point than at the free surface point.

Pipes Under Bending Loads

The normalized stress-intensity factors as a function of the parametric angle (ϕ) are shown in Figure 10 for a pipe ($R/t = 2$) subjected to remote bending with a semi-circular crack for various values of a/t. For this crack shape, the deeper cracks (larger a/t ratios) produced larger normalized stress-intensity factors where the crack meets the free surface but smaller values at the maximum depth point ($\phi = \pi/2$).

Rods Under Tension Loads

Figure 11 shows the normalized stress-intensity factors as a function of the parametric angle (ϕ) for a rod with various shape surface cracks with $a/D = 0.2$. When a/c was unity, the maximum normalized stress-intensity factor occurred at the free surface. When a/c was equal to 0.6, the maximum was at the deepest point. For surface cracks with an a/c ratio of 0.8, however, the normalized stress-intensity factors are nearly constant, much like the pipe.

Rods Under Bending Loads

The normalized stress-intensity factors as a function of the parametric angle (ϕ) for a rod with various shape surface cracks with $a/D = 0.2$ are shown in Figure 12. The maximum normalized stress-intensity factor occurred at the free surface for $a/c = 1$ and $a/c = 0.8$. For surface cracks with $a/c = 0.6$, however, the normalized stress-intensity factors all along the crack front are nearly constant.

Comparisons With Other Solutions

The comparison of the present results with those from the literature are difficult because, at least, three definitions of crack shapes have been used. All definitions differ in how the crack length c is measured. In this

paper, c is measured as the arc length, as shown in Figure 4. In some reports, c is measured as the horizontal projection of point B on the x-axis, while in other reports, c is defined as the intersection point of an ellipse with the x-axis. In the latter case, the crack front will not intersect the free suface at a right angle. The crack front shape, in the latter case, therefore, will be different from that used in this paper. In view of these difficulties, only a few comparisons can be made.

As previously mentioned, stress-intensity factor analyses of circumferential surface cracks in pipes have received very little attention in the literature. Delale and Erdogan [6] obtained stress-intensity factors for interior and exterior circumferential surface cracks and German, et al. [7] obtained stress-intensity factors for interior circumferential surface cracks by using the line-spring model. Most of the external circumferential surface crack configurations presented in Reference 6 were vastly different from the configurations presented in this paper. However, one configuration with $a/c = 0.775$, $a/t = 0.8$ and $R/t = 5.374$ falls within the range of parameters considered in this paper. (In the notation of Ref. 6, this configuration has $L_o/h = 0.8$, $a/h = 1$ and $\lambda_2 = 0.75$.) The normalized stress-instensity factor at the deepest point ($\phi = \pi/2$) of the crack was computed from the results of Reference 6 as 1.276. Interpolating the present results in Table 1, the normalized stress-intensity factor F_A for this configuration was found to be 1.161. The result from the line-spring model, reference 6, is about 10 percent higher than the present result.

The rod configurations with surface cracks subjected to remote tension have received more attention in the literature than the pipe configurations. These configurations were analyzed by Wilhem, et al. [1], Athanassiadis, et al. [3], and Nezu, et al. [4]. The present results are compared with the

results from References 1 and 3. Comparisons with the results from Nezu, et al. [4] could not be made because the crack shapes analyzed in Reference 4 and those in the present analysis (see Fig. 6) were very different.

Figure 13 compares the normalized stress-intensity factors at the free surface (F_B) and the maximum depth point (F_A) for a surface crack with $a/c = 0.6$ from the present finite-element analysis with those from a Boundary Integral Equation (BIE) method [3]. The results of Athanassiadis, et al. [3] were interpolated and plotted in Figure 13 as open symbols. The present results are shown by solid symbols. The normalized stress-intensity factors obtained by the BIE method were 0 to 10 percent lower than the present results.

Figure 14 compares the normalized stress-intensity factors at the maximum depth point for surface cracks with various shapes (a/c) and sizes (a/D) from the present analyses and from experimental results. Wilhem, et al. [1] obtained an experimental stress-intensity factor solution using the James-Anderson procedure [2]. These results are shown by the dashed curve in Figure 14. For the surface cracks in their tests, the a/c ratios varied from 0.95 to 0.85. The present results (symbols) for $a/c = 0.8$ and 1.0 bound the experimental results for $a/D < 0.25$ and are a little below for $a/D > 0.25$.

Bush [12] considered cracks with straight fronts (see insert in Fig. 14) in rods subjected to remote tension. He obtained stress-intensity factors from experimental compliance for these straight through cracks of various depths. His results are shown in Figure 14 by a solid curve. For a surface crack with an a/c ratio of 0.6 and an a/D ratio of 0.35 (see Fig. 6(c)), the crack configuration is very nearly the same as that for a crack with a straight front. For this configuration, the present results for $a/c = 0.6$ are a little below (about 2 percent) the straight through crack results. The

present results need not necessarily agree with the experimental results because the crack shapes are not identical, as noted previously.

CONCLUDING REMARKS

Stress-intensity factors for circumferential surface cracks in pipes and rods have been obtained by a three-dimensional finite-element analysis. The pipes and rods were subjected to either remote tension or remote bending loading. The surface cracks were nearly semi-elliptical and were oriented on a plane normal to the axis of pipes or rods. A wide range of crack shapes, crack sizes, and internal radius-to-wall thickness ratios have been considered. For each of these crack configurations and loadings, the stress-intensity factors calculated by the finite element analysis are presented.

Stress-intensity factors for surface cracks in a pipe were found to be insensitive to internal radius-to-wall thickness (R/t) ratios ranging from 1 to 10, for crack depth-to-length (a/c) ratios ranging from 0.8 to 1.0 with crack depth-to-wall thickness (a/t) ratios less than 0.8. For $a/c = 0.6$ and $a/t = 0.8$, however, the stress-intensity factors showed significant variation with R/t. The effect of the curvature of the pipe (R/t) is to elevate the stress-intensity factors compared to a flat plate ($R/t = \infty$). This effect is more pronounced at the deepest point than at the free surface point.

Stress-intensity factors for a surface crack in a rod were 0 to 10 percent higher than those calculated from a boundary-integral analysis. The stress-intensity factors agreed well with experimental results for surface cracks in rods and approached the experimental results for cracks with straight fronts.

The stress-intensity factors obtained here should be useful in predicting fatigue-crack growth and fracture of surface cracks in cylinders and rods.

Acknowledgements

The authors gratefully acknowledge the support of this effort by Mr. Royce Forman of the NASA Lyndon B. Johnson Space Center (Shuttle Operations - Engineering and Test Support) and by Dr. J. H. Crews, Jr. of the NASA Langley Research Center (Materials Division). This work was performed as a part of the contracts NAS1-17090 and NAS1-17683.

APPENDIX

The purpose of this appendix is to present the procedure used to develop finite-element models for surface cracks in pipe and rod configurations through a conformal transformation.

A cylinder with a surface crack is shown in Figure 15(a). The stress-intensity factors for this configuration were evaluated from a nodal-force method [9]. In this method, the nodal forces normal to the crack plane (x,y plane) and ahead of the crack front are used. The nodal- force method also requires that these forces be evaluated at nodes which are very near the crack front and which lie on lines in the x,y plane that are normal to the crack front. Therefore, the finite-element model should be such that the normality at the crack front is maintained. This is achieved through a conformal transformation as follows.

First, a finite-element model for a semi-elliptical surface crack with semi-minor and semi-major axes, a' and c', respectively, in a plate of width w' and a thickness of t' (see Fig. 15(b)) is developed such that

$$a' = \ln\left(\frac{R + t}{R + t - a}\right) \tag{3}$$

$$c' = \frac{C}{R + t} \tag{4}$$

and

$$t' = \ln \frac{R + t}{R} \tag{5}$$

To obtain the desired configuration in Figure 15(a), a conformal transformation

$$x = (R + t)\, e^{-y'} \cos(w'/4 - x') \tag{6}$$

$$y = (R + t)[1 - e^{-y'} \sin(w'/4 - x') \tag{7}$$

$$z = z'$$

and

$$w' = 2\pi \tag{8}$$

is used. This transformation transforms every point in the x',y',z' system to a unique point in the x,y,z system and maintains normality. Because the finite-element model of a surface crack in a flat plate (Fig. 15(b)) has nodes along hyperbolas near the crack front [11] (and, hence, normality to the semi-elliptical crack front in the x',y' plane is assured), the conformal transformation gives nodes along curves in the x,y plane which are also normal to the crack front in the pipe configuration (Fig. 15(a)).

The finite-element models for the surface crack in the rod configuration were obtained from the pipe models by idealizing the inside core with finite elements (see Fig. 2).

REFERENCES

[1] Wilhem, D.; Fitzgerald, J.; Carter, J. and Dittmer, D., "An Empirical Approach to Determining K for Surface Cracks," International Conference of Fracture (ICF-5), Advances in Fracture Research, Vol. 1, March 1981, D. Francois, editor, pp. 11-21.

[2] James, L. A. and Anderson, W. E., "A Simple Procedure for Stress Intensity Factor Calibration," Engineering Fracture Mechanics Journal, Vol. 1, 1969, pp. 565-568.

[3] Athanassiadis, A.; Boissenot, J. M., Brevet, P., Francois, D. and Raharinaivo, A., "Linear Elastic Fracture Mechanics Computations of Cracked Cylindrical Tensioned Bodies," International Journal of Fracture, Vol. 17, No. 6, December 1981, pp. 553-566.

[4] Nezu, K.; Machida, S. and Nakamura, H., "SIF of Surface Cracks and Fatigue Crack Propagation Behaviour in a Cylindrical Bar," The 25th Japan Congress on Materials Research - Metallic Materials," March 1982, pp. 87-92.

[5] Trantina, G. G.; deLorenzi, H. G. and Wilkening, W. W., "Three-Dimensional Elastic-Plastic Finite Element Analysis of Small Surface Cracks," Engineering Fracture Mechanics, Vol. 18, No. 5, 1983, pp. 925-938.

[6] Delale, F. and Erdogan, F., "Application of Line-Spring Model to a Cylindrical Shell Containing a Circumferential or Axial Part-Through Crack," Journal of Applied Mechanics, Vol. 49, March 1982, pp. 97-102.

[7] German, M. D.; Kumar, V.; and deLorenzi, H. G., "Analysis of Surface Cracks in Plates and Shells Using the Line-Spring Model and Adina," Computers and Structures, Vol. 17, No. 5-6, 1983, pp. 881-890.

[8] Forman, R. G. and Shivakumar, V., "Growth Behavior of Surface Cracks in the Circumferential Plane of Solid and Hollow Cylinders," presented at the Seventeenth National Symposium on Fracture Mechanics, August 7-9, 1984, Albany, New York.

[9] Raju, I. S. and Newman, J. C., Jr., "Three-Dimensional Finite-Element Analysis of Finite-Thickness Fracture Specimens," NASA TN D-8414, 1977.

[10] Raju, I. S. and Newman, J. C., Jr., "Improved Stress-Intensity Factors for Semi-Elliptical Surface Cracks in Finite-Thickness Plates," NASA TM X-72825, 1977.

[11] Raju, I. S. and Newman, J. C., Jr., "Stress-Intensity Factors for a Wide Range of Semi-Elliptical Surface Cracks in Finite-Thickness Plates," Engineering Fracture Mechanics, Vol. 11, No. 4, 1979, pp. 817-829.

[12] Bush, A. J., "Stress-Intensity Factors for Single-Edge-Crack Solid and Hollow Round Bars Loaded in Tension," Journal of Testing and Evaluation, JTEVA. Vol. 9, No. 4, July 1981, pp. 216-223.

Table 1.- Normalized stress-intensity factor, $K/S_t\sqrt{\pi a/Q}$, for surface crack in a pipe subjected to tension loads.

A = maximum depth point
B = free surface point

a/c = 1.0						
$\frac{R}{t}$	a/t = 0.2		a/t = 0.5		a/t = 0.8	
	A	B	A	B	A	B
1	1.015	1.160	1.036	1.237	1.076	1.385
2	1.017	1.157	1.041	1.235	1.072	1.383
4	1.019	1.154	1.046	1.234	1.072	1.381
10	1.020	1.152	1.049	1.233	1.074	1.380
a/c = 0.8						
$\frac{R}{t}$	a/t = 0.2		a/t = 0.5		a/t = 0.8	
	A	B	A	B	A	B
1	1.061	1.060	1.114	1.161	1.202	1.354
2	1.059	1.056	1.106	1.155	1.174	1.331
4	1.058	1.053	1.103	1.156	1.157	1.333
10	1.057	1.051	1.101	1.156	1.144	1.335
a/c = 0.6						
$\frac{R}{t}$	a/t = 0.2		a/t = 0.5		a/t = 0.8	
	A	B	A	B	A	B
1	1.113	0.943	1.226	1.080	1.455	1.327
2	1.105	0.937	1.194	1.070	1.342	1.285
4	1.101	0.933	1.178	1.071	1.285	1.285
10	1.097	0.930	1.167	1.070	1.247	1.290

Table 2.- Normalized stress-intensity factor, $K/S_b\sqrt{\pi a/Q}$, surface crack in a pipe subjected to bending loads.

A = maximum depth point
B = free surface point

a/c = 1.0						
$\frac{R}{t}$	a/t = 0.2		a/t = 0.5		a/t = 0.8	
	A	B	A	B	A	B
1	0.943	1.136	0.856	1.162	0.777	1.233
2	0.966	1.137	0.919	1.188	0.870	1.287
4	0.981	1.133	0.971	1.204	0.950	1.327
10	0.995	1.131	1.012	1.212	1.019	1.348
a/c = 0.8						
$\frac{R}{t}$	a/t = 0.2		a/t = 0.5		a/t = 0.8	
	A	B	A	B	A	B
1	0.989	1.037	0.931	1.079	0.885	1.162
2	1.007	1.037	0.984	1.107	0.966	1.224
4	1.021	1.033	1.028	1.126	1.033	1.276
10	1.032	1.032	1.064	1.136	1.088	1.303
a/c = 0.6						
$\frac{R}{t}$	a/t = 0.2		a/t = 0.5		a/t = 0.8	
	A	B	A	B	A	B
1	1.042	0.919	1.034	0.980	1.094	1.078
2	1.056	0.919	1.069	1.015	1.118	1.152
4	1.065	0.916	1.102	1.039	1.155	1.220
10	1.071	0.913	1.130	1.051	1.188	1.257

Table 3.- Normalized stress-intensity factor, $K/S\sqrt{\pi a/Q}$, for surface crack in a rod subjected to tension or bending loads.

A = maximum depth point
B = free surface point

Tension loads						
$\frac{a}{D}$	a/c = 1.0		a/c = 0.8		a/c = 0.6	
	A	B	A	B	A	B
0.05	1.012	1.156	1.056	1.054	1.107	0.933
0.125	1.015	1.189	1.083	1.101	1.176	0.999
0.20	1.038	1.260	1.131	1.200	1.316	1.129
0.275	1.087	1.356	1.227	1.335	1.565	1.329
0.35	1.175	1.475	1.387	1.509	1.835	1.516
Bending loads						
$\frac{a}{D}$	a/c = 1.0		a/c = 0.8		a/c = 0.6	
	A	B	A	B	A	B
0.05	0.938	1.129	0.984	1.029	1.035	0.907
0.125	0.836	1.114	0.901	1.019	0.987	0.903
0.20	0.749	1.112	0.830	1.028	0.985	0.909
0.275	0.683	1.109	0.795	1.040	1.041	0.924
0.35	0.629	1.106	0.782	1.039	1.056	0.876

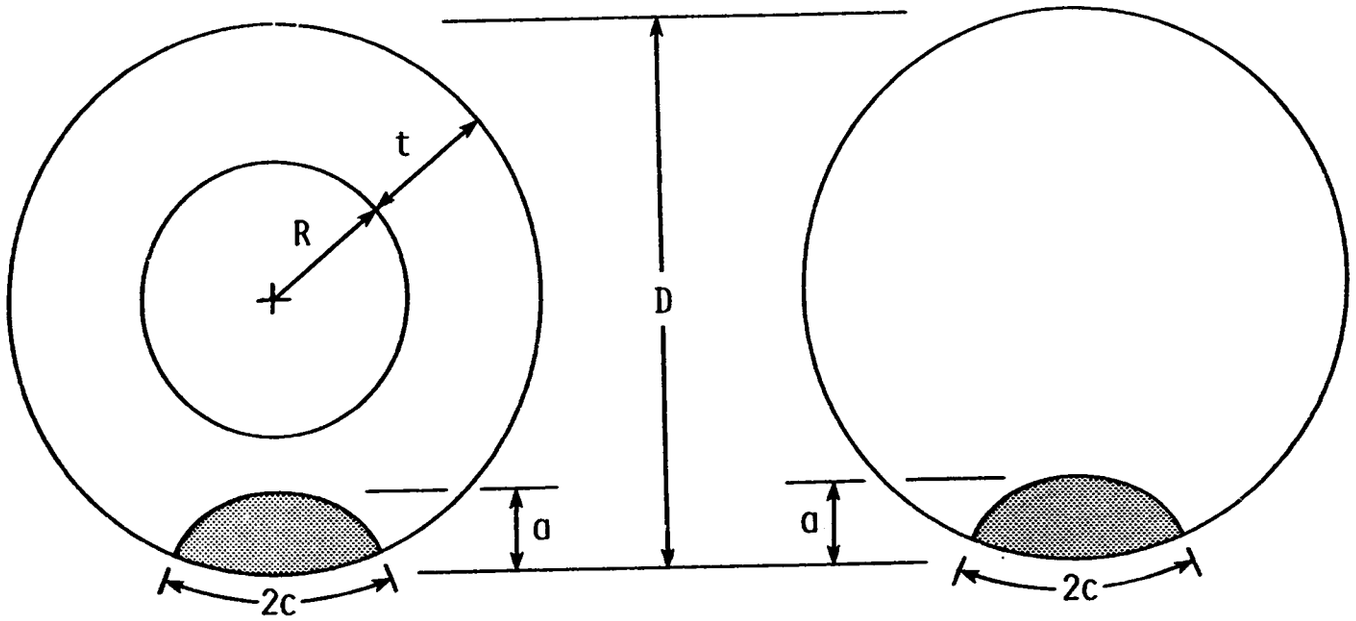

(a) Pipe.

(b) Rod.

Fig. 1.- Surface crack in a pipe and a rod.

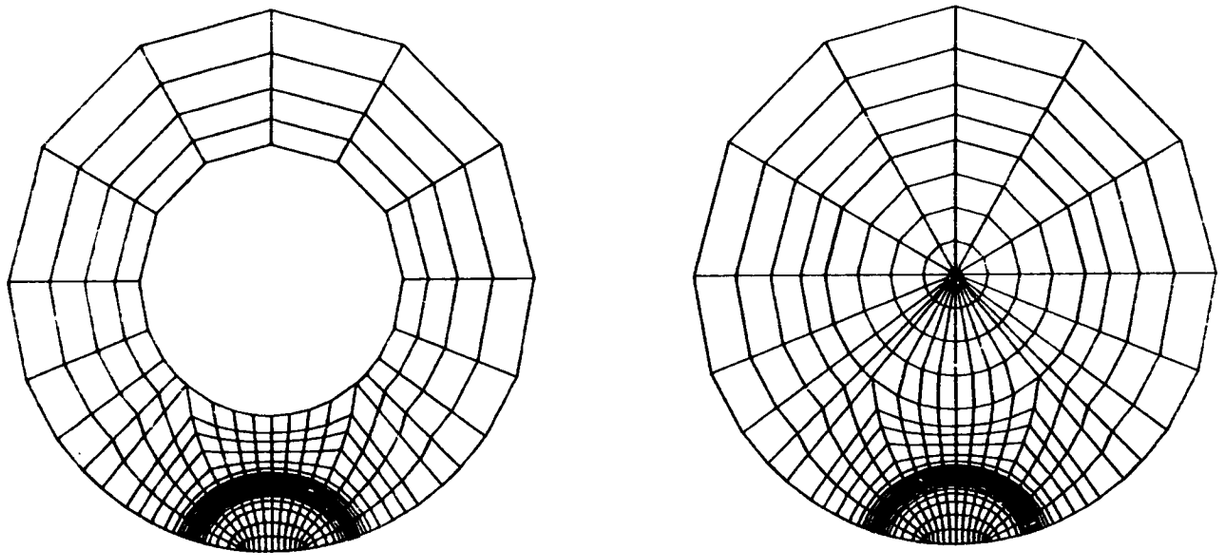

(a) Pipe.

(b) Rod.

Fig. 2.- Finite-element idealizations of a surface crack in a pipe and a rod.

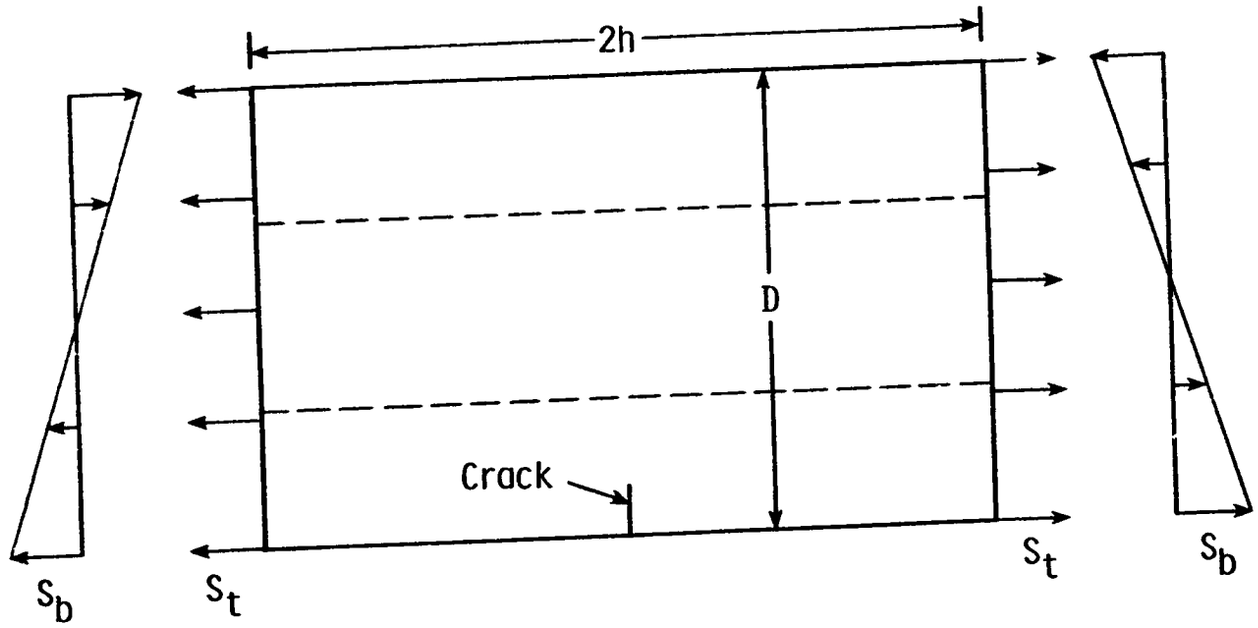

Fig. 3.- Loading applied to the pipe and rod.

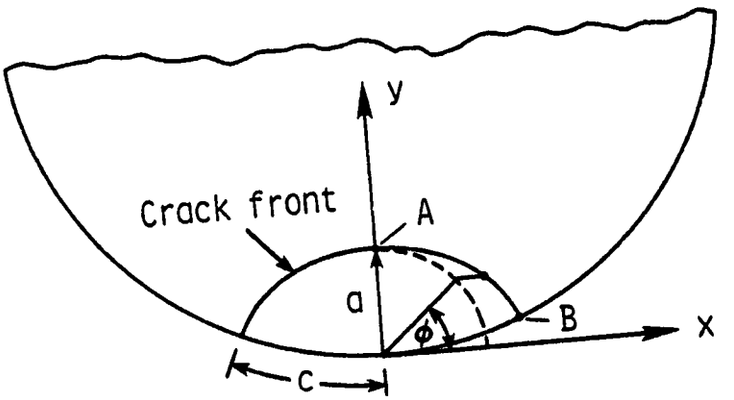

Fig. 4.- Coordinate system and dimensions for surface crack.

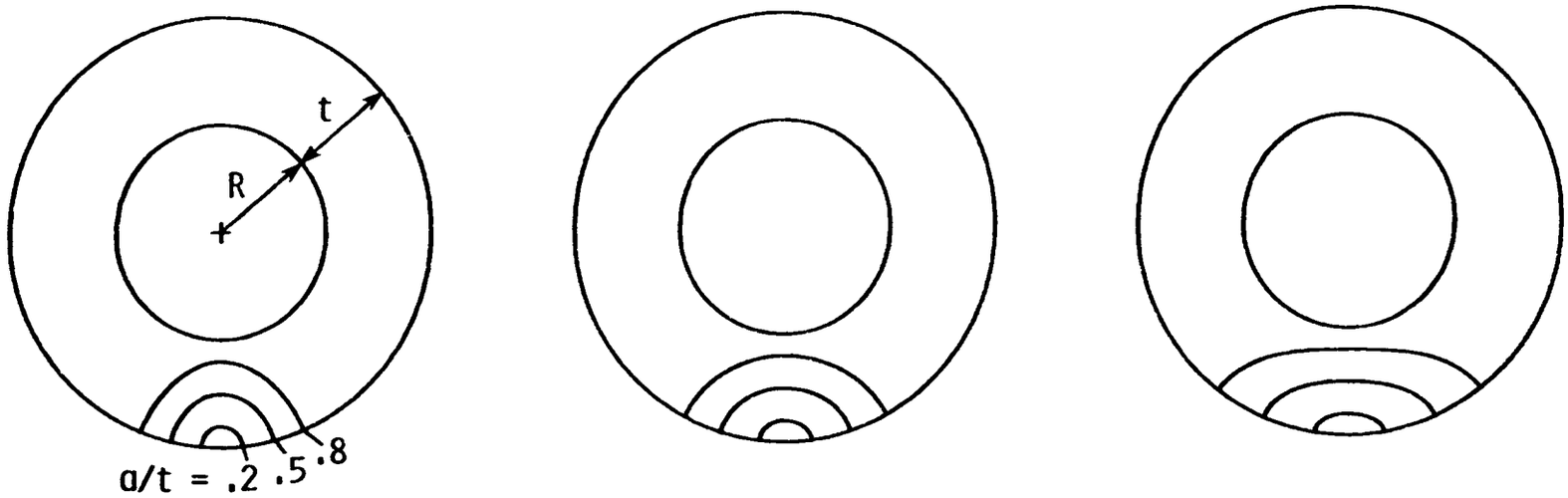

Fig. 5.- Surface-crack shapes and sizes analyzed for the pipe.

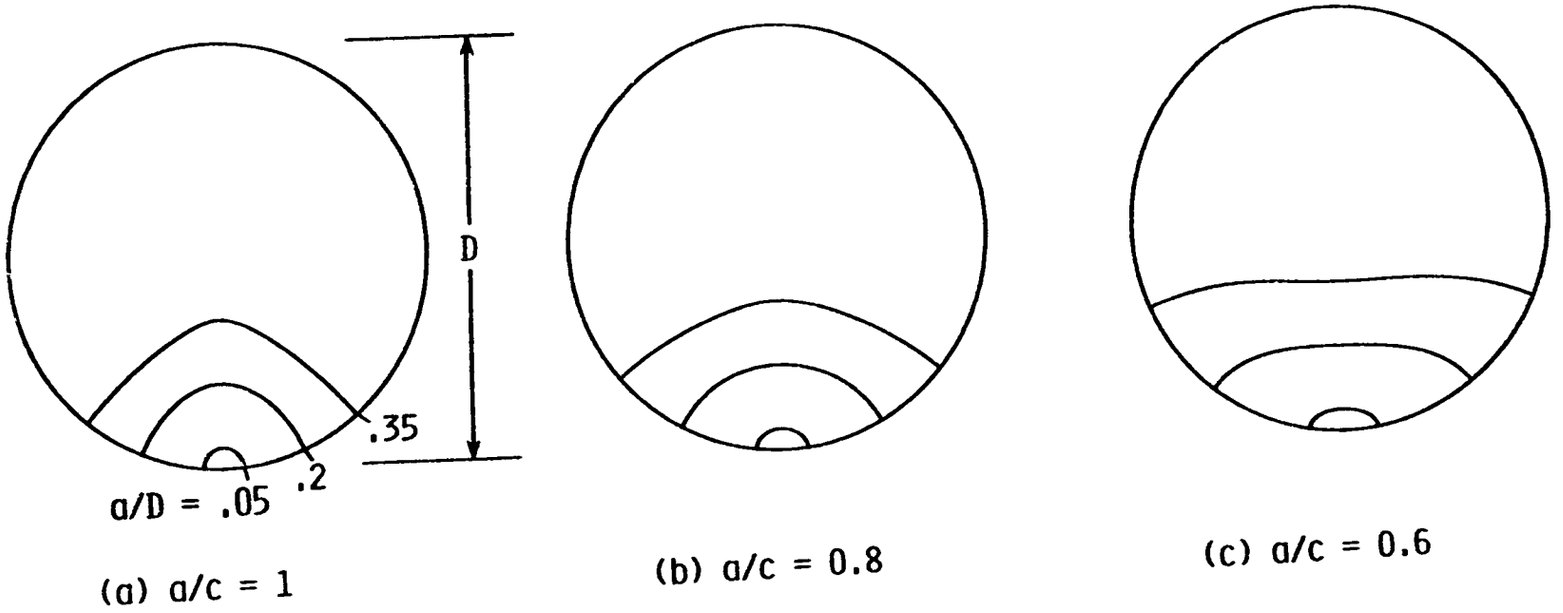

Fig. 6.- Surface-crack shapes and sizes analyzed for the rod.

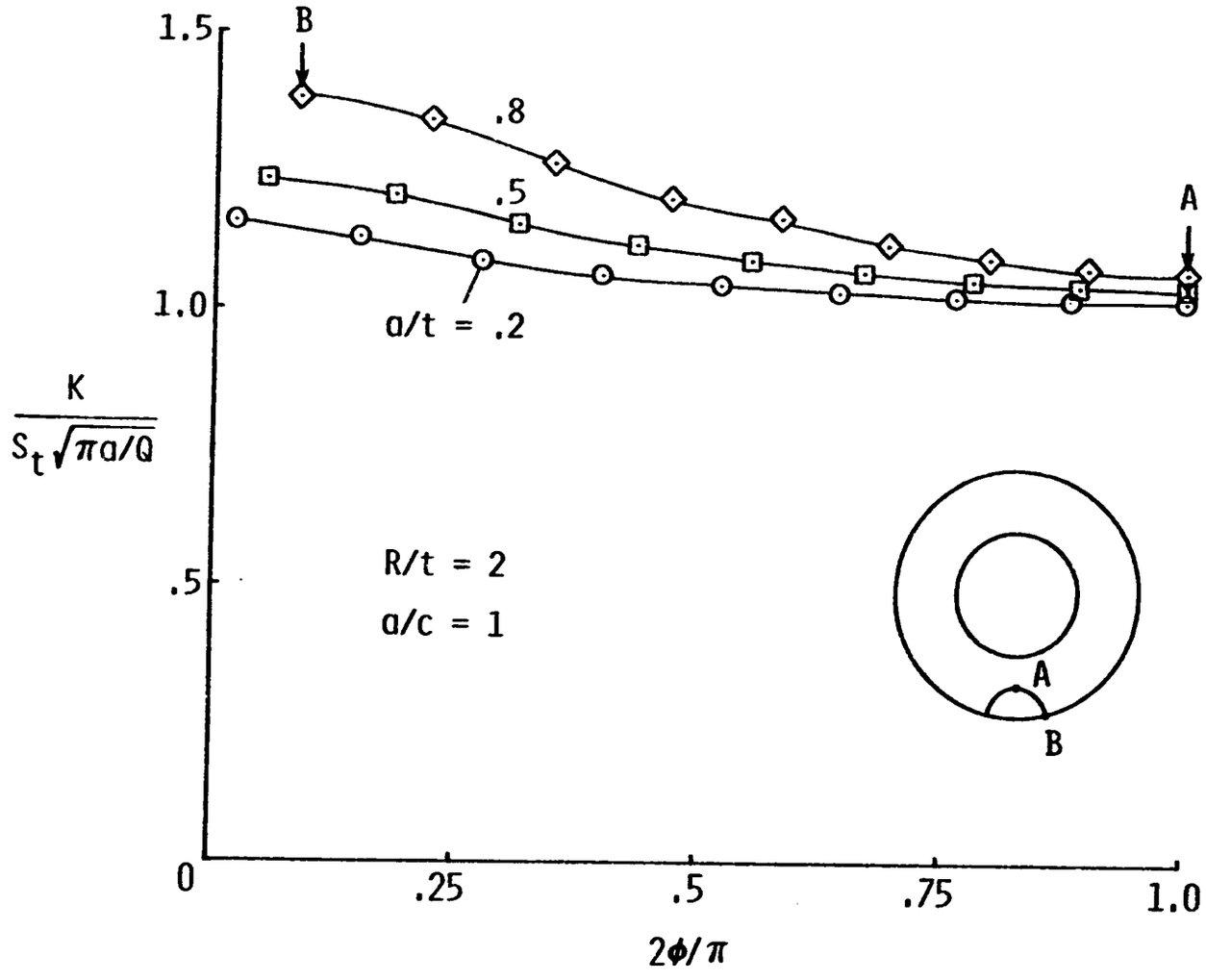

Fig. 7.- Normalized stress-intensity factors along the front of a surface crack (a/c = 1) in a pipe under tension.

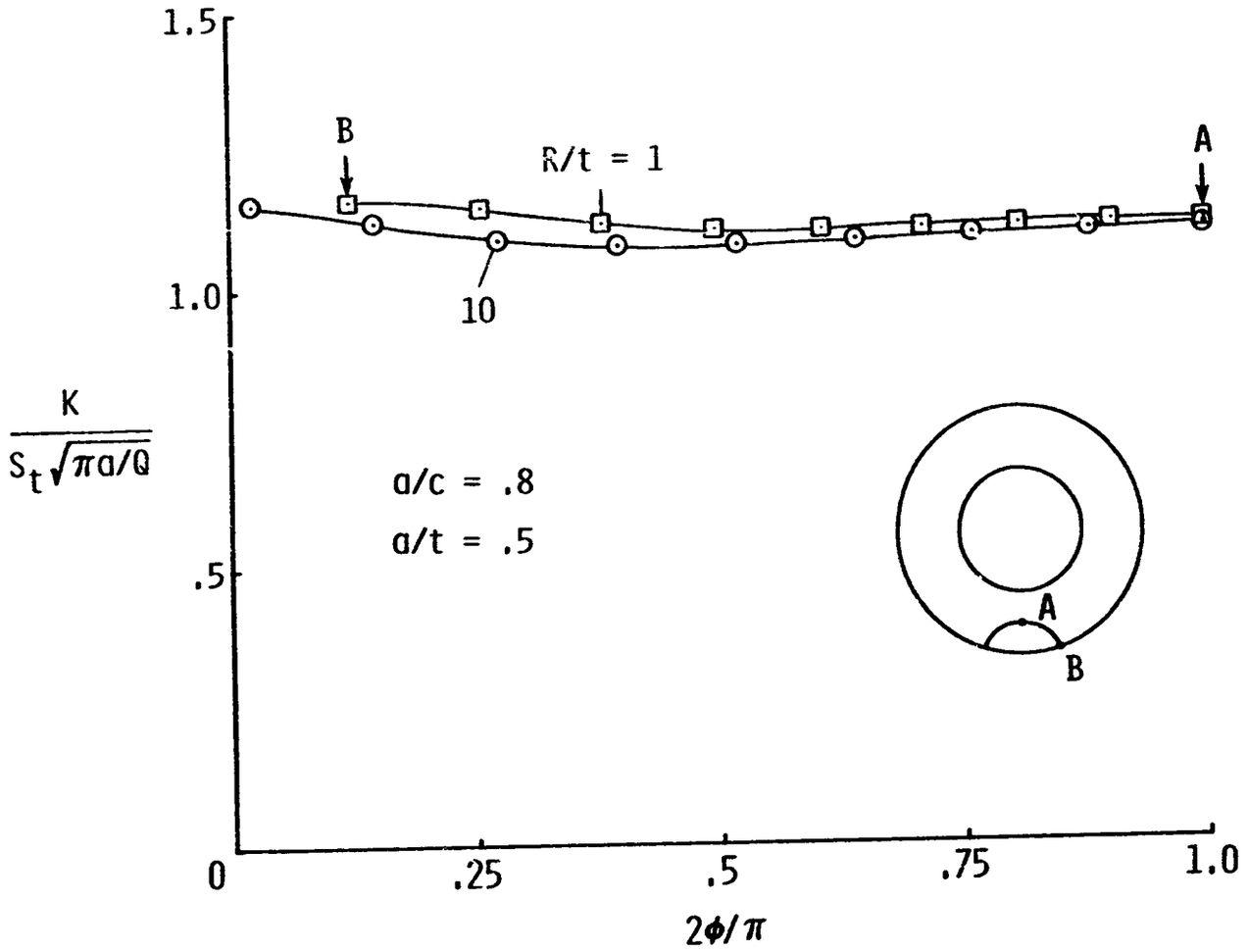

Fig. 8.- Normalized stress-intensity factors along the front of a surface crack (a/c = 0.8) in a pipe under tension.

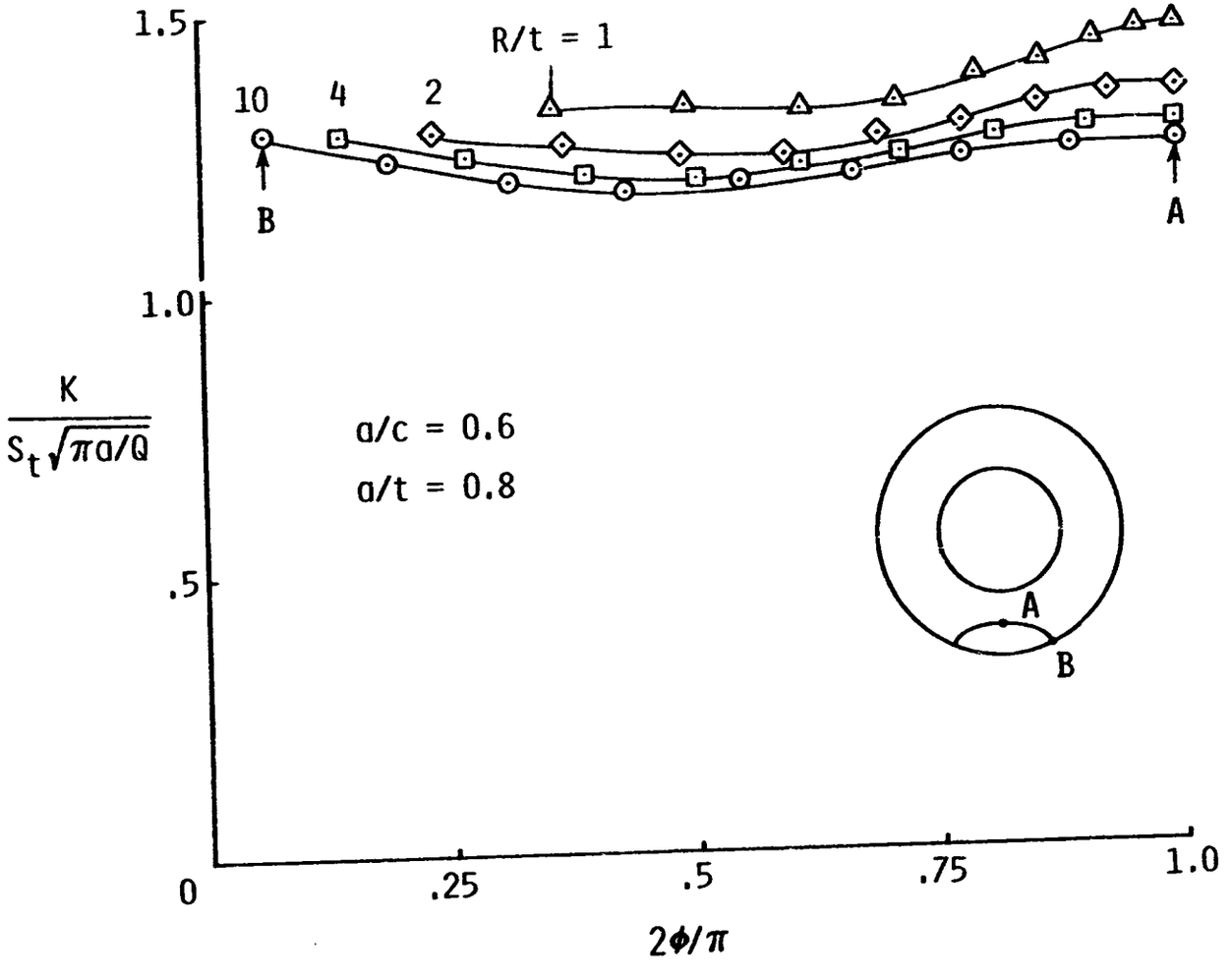

Fig. 9.- Normalized stress-intensity factors along the front of a deep surface crack (a/c = 0.6) in a pipe under tension.

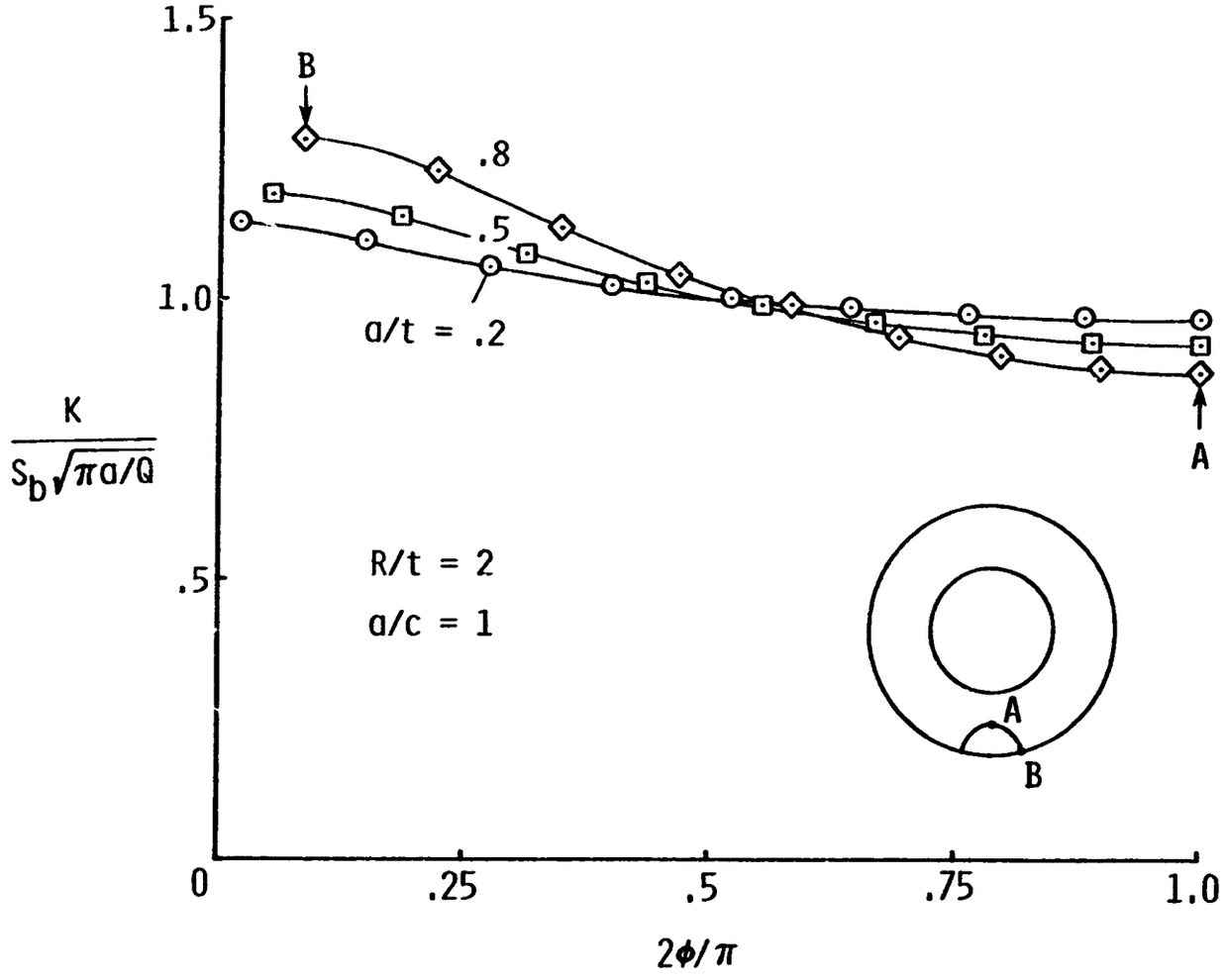

Fig. 10.- Normalized stress-intensity factors along the front of a surface crack (a/c = 1) in a pipe under bending.

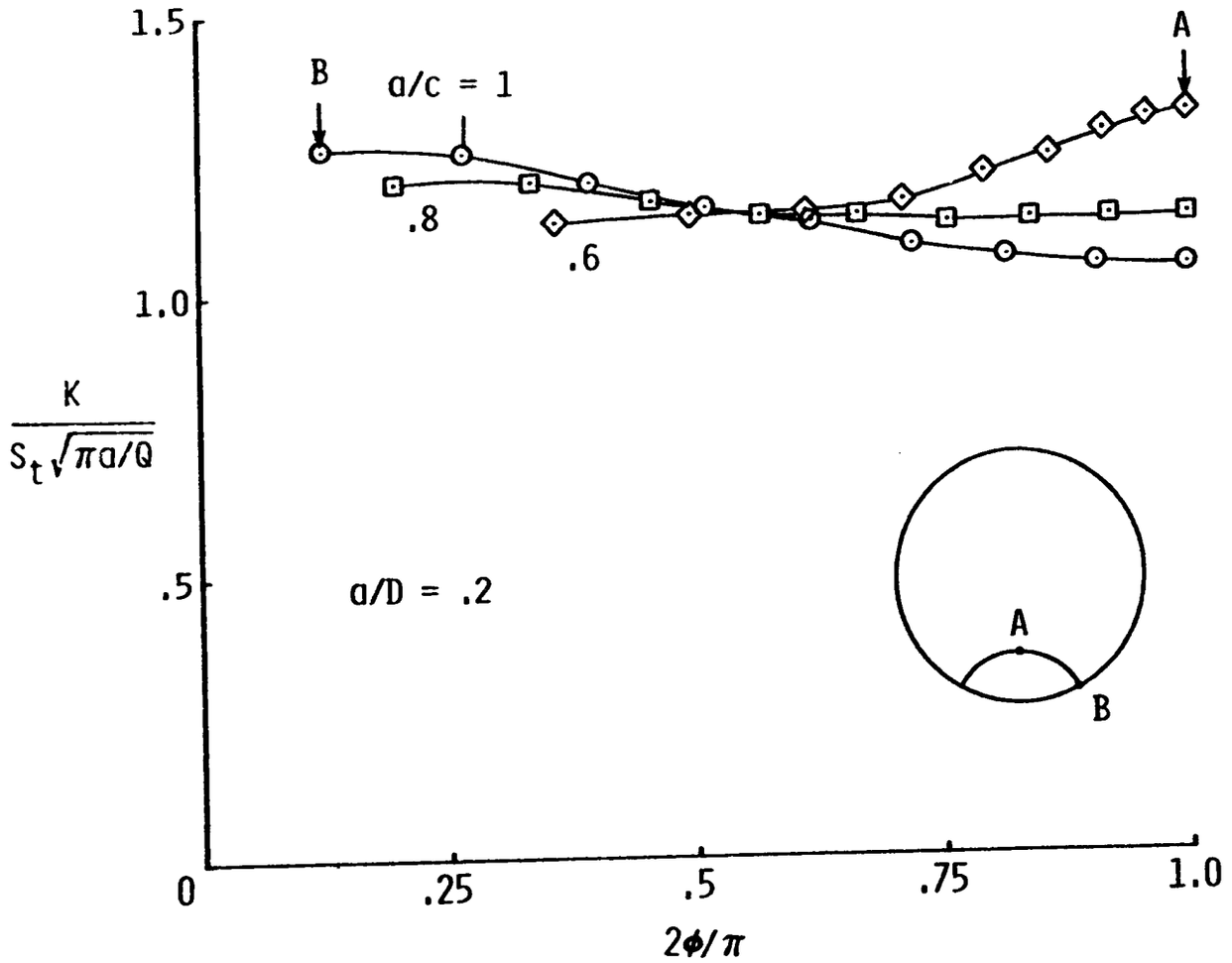

Fig. 11.- Normalized stress-intensity factors along the front of various shape surface cracks in a rod under tension.

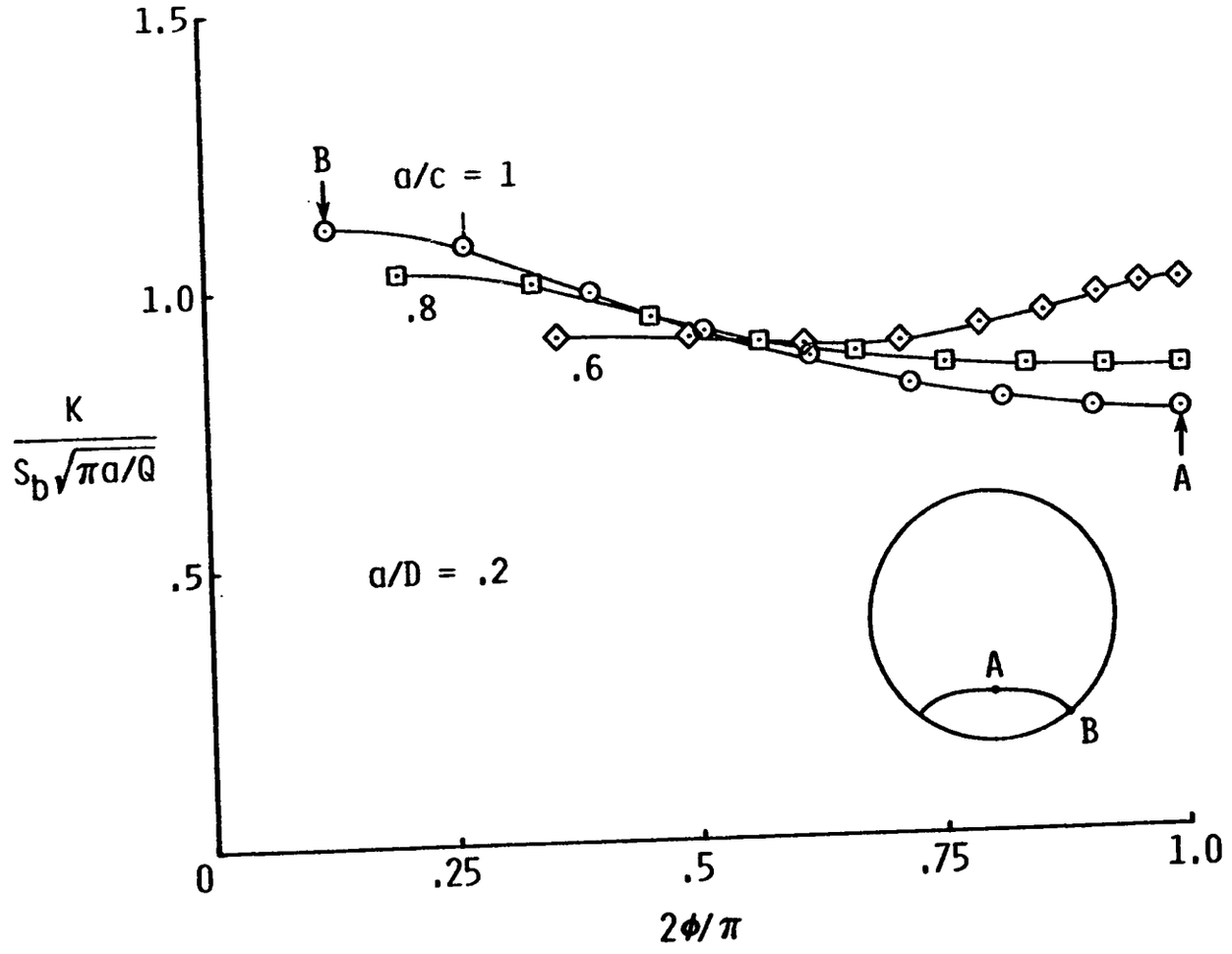

Fig. 12.- Normalized stress-intensity factors along the front of various shape surface cracks in a rod under bending.

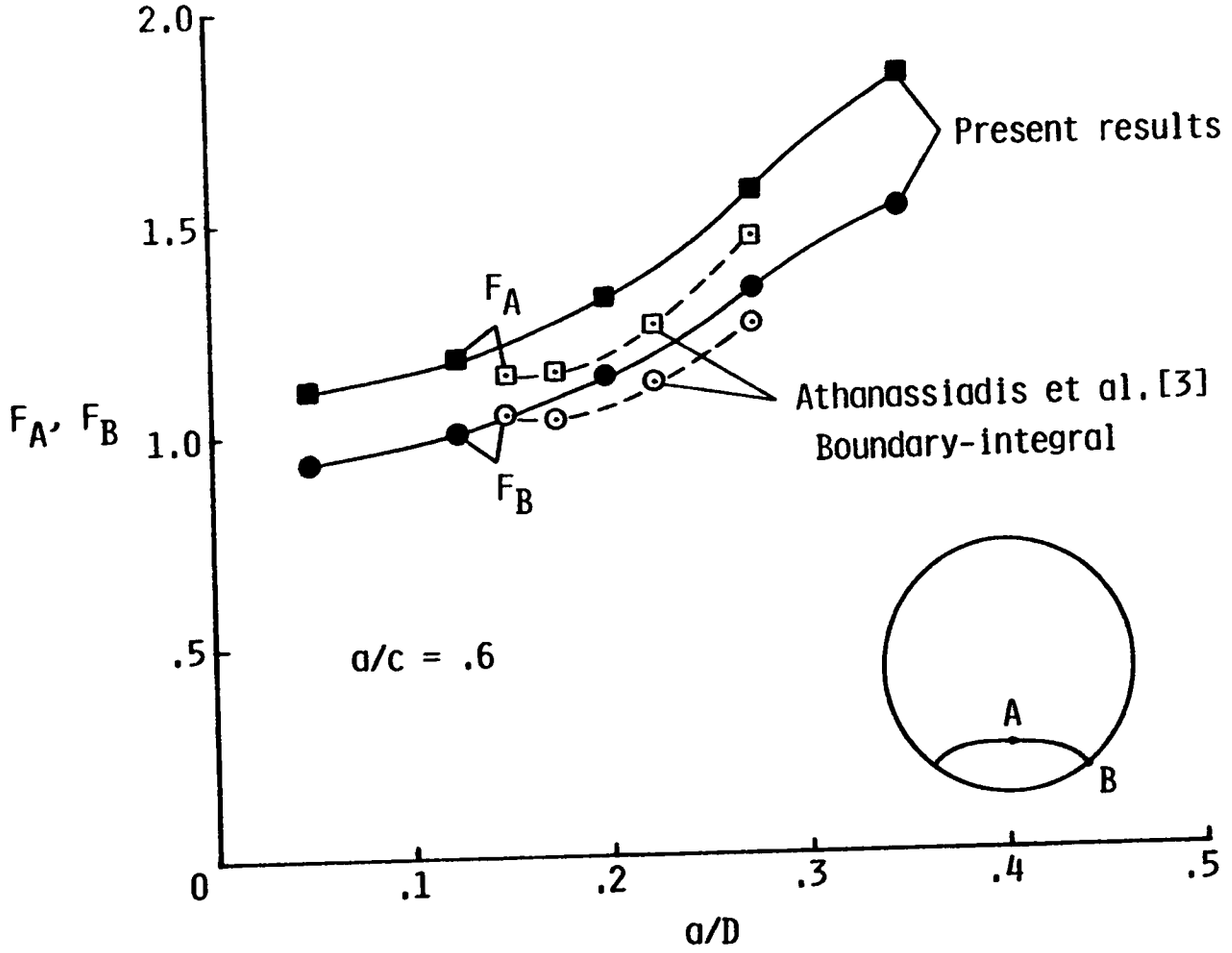

Fig. 13.- Comparison of boundary-correction factors for a surface crack in a r under tension.

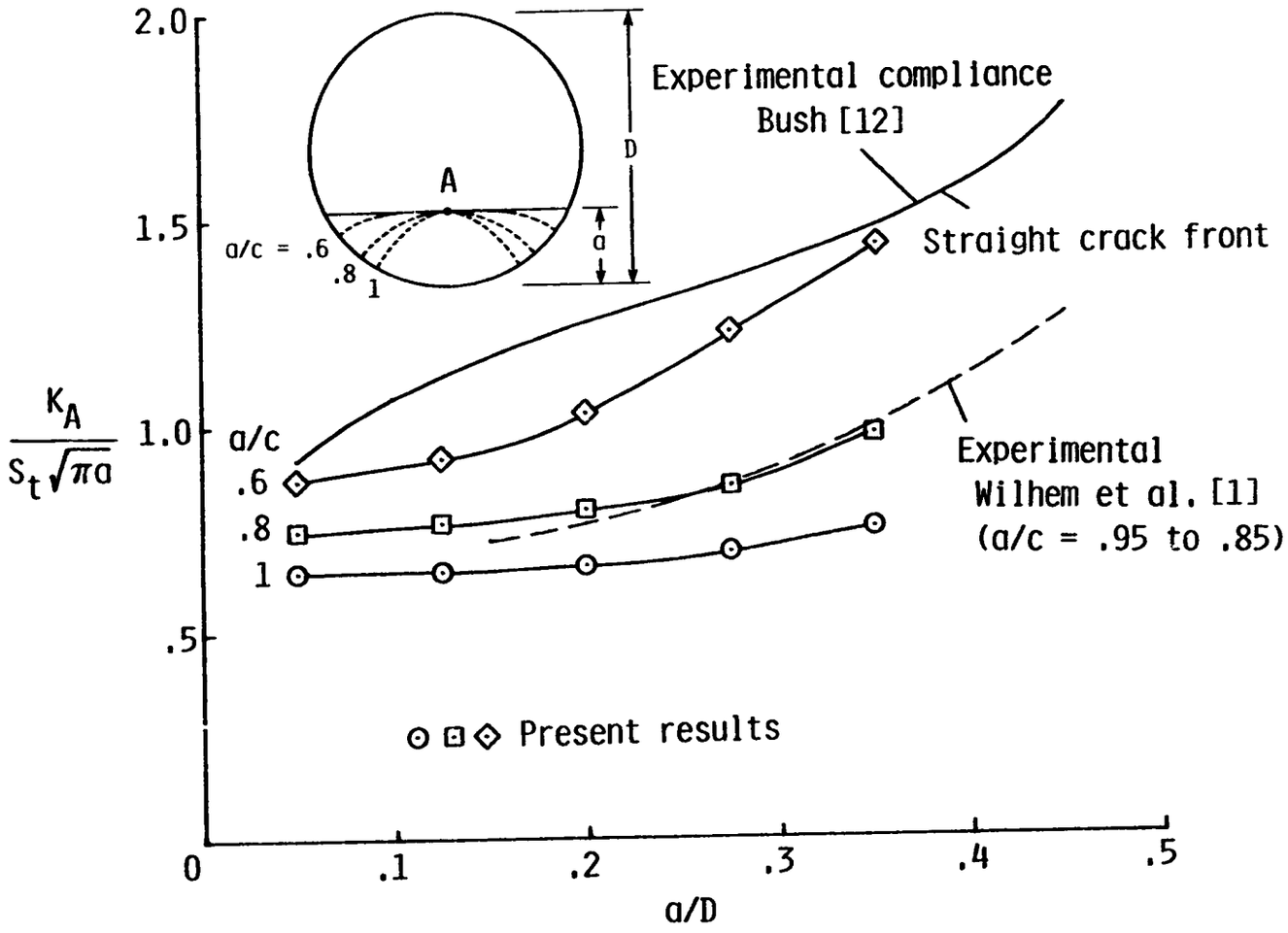

Fig. 14.- Comparison of experimental and calculated stress-intensity factors for a surface crack in a rod under tension.

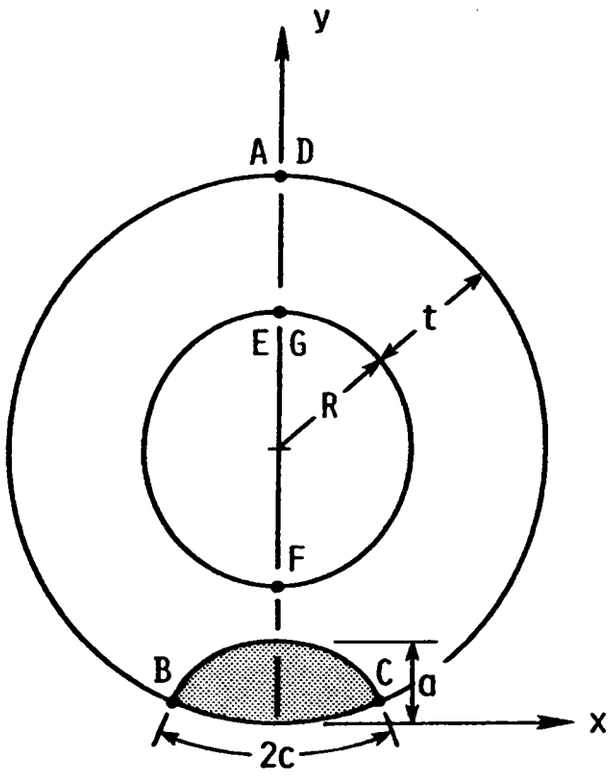

(a) Surface crack in pipe.

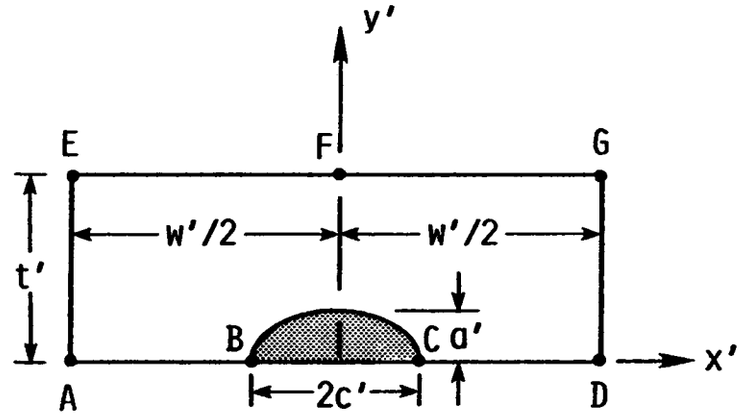

(b) Surface crack in plate.

Fig. 15.- Conformal transformation of a surface crack in a plate to a surface crack in a pipe.

1. Report No.	2. Government Accession No.	3. Recipient's Catalog No.
NASA TM-87594		

4. Title and Subtitle	5. Report Date
Stress-Intensity Factors for Circumferential Surface Cracks in Pipes and Rods Under Tension and Bending Loads	August 1985
	6. Performing Organization Code 505-33-23
7. Author(s)	8. Performing Organization Report No.
I. S. Raju* and J. C. Newman, Jr.	
	10. Work Unit No.
9. Performing Organization Name and Address	
NASA Langley Research Center Hampton, VA 23665-5225	11. Contract or Grant No.
	13. Type of Report and Period Covered
12. Sponsoring Agency Name and Address	Technical Memorandum
National Aeronautics and Space Administration Washington, DC 20546-0001	14. Sponsoring Agency Code

15. Supplementary Notes

*Analytical Services & Materials, Inc., Tabb, VA 23602

16. Abstract

The purpose of this paper is to present stress-intensity factors for a wide range of nearly semi-elliptical surface cracks in pipes and rods. The surface cracks were oriented on a plane normal to the axis of pipes or rods. The configurations were subjected to either remote tension or bending loads. For pipes, the ratio of crack depth to crack length (a/c) ranged from 0.6 to 1; the ratio of crack depth to wall thickness (a/t) ranged from 0.2 to 0.8; and the ratio of internal radius to wall thickness (R/t) ranged from 1 to 10. For rods, the ratio of crack depth to crack length also ranged from 0.6 to 1; and the ratio of crack depth to rod diameter (a/D) ranged from 0.05 to 0.35. These particular crack configurations were chosen to cover the range of crack shapes (a/c) that have been observed in experiments conducted on pipes and rods under tension and bending fatigue loads. The stress-intensity factors were calculated by a three-dimensional finite-element method. The finite-element models employed singularity elements along the crack front and linear-strain elements elsewhere. The models had about 6500 degrees of freedom. The stress-intensity factors were evaluated using a nodal-force method.

The present results were compared with other analytical and experimental results for some of the crack configurations. the results generally agreed within 10 percent.

17. Key Words (Suggested by Author(s))	18. Distribution Statement
Cracks, surface cracks, rods, pipes, crack propagation, fracture, stress analysis, finite elements, stress-intensity factors	Unclassified - Unlimited Subject Category 39

19. Security Classif. (of this report)	20. Security Classif. (of this page)	21. No. of Pages	22. Price
Unclassified	Unclassified	35	A03

NASA-305 For sale by the National Technical Information Service, Springfield, Virginia 22161